วิธีออกแบบผนังชั้นในสุด ของเตาปฏิกรณ์ฟิวชันสำหรับอิออนเบา

A Mechanical Design of Primary Enclosure for Light Ion Beam (LIB) Fusion Reactors

อภิวันท์ พลชัย
APIWON POLCHAI

ภาควิชาวิศวกรรมเครื่องกล คณะวิศวกรรมศาสตร์ มหาวิทยาลัยเชียงใหม่
Mechanical Engineering Department, Chiang Mai University

บทคัดย่อ

ในเอกสารนี้ เป็นการพัฒนาวิธีการคำนวณอย่างเป็นขั้นตอน สำหรับการหาอาการตอบสนองของผนังชั้นในสุดของเตาปฏิกรณ์ฟิวชันสำหรับอิออนเบา โดยภาระซึ่งกระทำต่อผนังเป็นความดันที่เกิดจากปฏิกิริยาฟิวชันที่ทราบขนาดและลักษณะแล้ว ได้เลือกใช้ผนังเป็นผิวของทรงกลม ซึ่งจะแบ่งออกเป็นผนังย่อยโดยเส้นเมอริเดียนและเส้นที่ขนานกับเส้นอีเควเตอร์ ผนังย่อยจะถูกวิเคราะห์โดยคิดว่าเป็นชิ้นส่วนเหมือนกับแผ่นเรียบที่มีเนื้อวัสดุตันและกลวง ซึ่งการคำนวณอาการตอบสนองเชิงพลวัตจะอาศัยแฟคเตอร์พลวัตช่วย ในที่สุดได้กำหนดกรรมวิธีในการคำนวณอย่างเป็นระเบียบขึ้นมาพร้อม ๆ กับเสนอกราฟบางอย่างของตัวแปรจำเป็นที่สำคัญ เพื่อใช้ในการออกแบบ เลือกขนาดของผนังย่อยภายใต้เงื่อนไขว่าความเค้น และ/หรือ ระยะแอ่นสูงสุดจะต้องไม่เกินขีดจำกัดที่กำหนดให้ ในที่นี้ยังได้เสนอตัวอย่างการคำนวณในการออกแบบจริงมาพอสังเขป จากผลที่แสดง พบว่ามิติของผนังย่อยพร้อมทั้งความเค้นและระยะแอ่นตัวสูงสุดที่เกิดขึ้น มีแนวโน้มและศักยภาพว่าจะใช้ได้จริงในทางปฏิบัติ

ABSTRACT

A technique is developed for the calculation of primary-enclosure responses for LIB fusion reactors. The load is a known inner pressure. A spheroidal shape is considered for the enclosure whose surface divided symmetrically by meridian lines together with lines parallel to equator. Subpanels of the shell are analyzed as plate-like components of solid and hollow geometries with appropriate dynamic load factors. A systematic procedure for calculation and some parametric curves are given for the determination of subpanel dimensions on the condition that the prescribed deflection and/or stress limit have to be satisfied. Sample calculations show that the results have great potential for designing of such reactor enclosure.

1. Introduction

Practically the design of the primary enclosure of a LIB fusion reactor is influenced by numbers of factors. For structural design purposes, the major load is a point source of repetitive blast-wave impinging on the wall, so a structural configuration having spherical characters would be generally natural. In addition, a conceptual ribbed shell is modelled with the assumption that the design of ribs and associated supporting members are left for others. The work which follows will focus on subpanels of the spheroid shell. Furthermore, it is assumed that shell temperature can be kept at near constant level by an appropriate cooling system so that material properties can be considered unchanged with time. In the analysis a subpanel is supported by meridianal ribs and by cross ribs, which will be considered as "simply supported" or "clamped". The rib structure must be chosen so that plate dimensions are small as compared to shell curvature. The details are shown in Figure 1(a), and Figure 4. Therefore, the classical flat-plate theory in bending can be applied. This is known to be a conservative approximation since we shall ignore any advantage from in-plane resistive forces which are transmitted by supporting structure. Additional approximation is also introduced without reducing accuracy to any significant degree. The studies of trapezoidal plates[1], [7] show that if tapering is very gradual, the plate can be considered as an equivalent rectangular shape. Referring to Figure 1(b), these conditions would be fulfilled for $b > 2a_2$ and $a_1 > 0.25\, a_2$. Hence, the following analysis of subpanels will be carried out on this ground.

2. Modal Shapes of Plates

Consider the rectangular plate whose configuration is shown in Figure 1(c). The study[3],[4] on natural vibration leads to the following results:

Case (1) : All edges are simply supported.

$$\text{Modal shape : } \sin\frac{m\pi x}{a}\ \sin\frac{n\pi y}{b};\ m,n = 1,2,3,....$$

Case (2) : Simply supported along $y = 0$, $y = b$; clamped along $x = 0$, $x = a$.

$$\text{Modal shape : } \{1-\cos\frac{2m\pi x}{a}\}\sin\frac{n\pi y}{b};\ m,n=1,2,3,....$$

Case (3) : All edges are clamped.

$$\text{Modal shape : } \{1-\cos\frac{2m\pi x}{a}\}\{1-\cos\frac{2n\pi x}{b}\};\ m,n=1,2,3,...$$

3. Dynamic Response of Plates

Here, all three cases, the plate will be acted upon by a time-dependent uniform pressure p(t) so that a short-period response w(x,y,t) can be considered as their first mode shape, i.e. m = 1, n = 1, multiplied by time-dependent coefficient x(t);

Case (1) := $w(x,y,t) = x_1(t)\sin\frac{\pi x}{a}\sin\frac{\pi y}{b}$

Case (2) := $w(x,y,t) = x_2(t)(1-\cos\frac{2\pi x}{a})\sin\frac{\pi y}{b}$,

Case (3) := $w(x,y,t) = x_3(t)$
$(1-\cos\frac{2\pi x}{a})(1-\cos\frac{2\pi y}{b})$,.....(1)

To obtain the modal equation of motion, Lagrange's equation[3] is employed :

$$\frac{d}{dt}\frac{\partial K}{\partial x} + \frac{\partial U}{\partial x} = \frac{\partial W}{\partial x} \quad .....(2)$$

The K is the total kinetic energy of plate, which is calculable from

$$K = \int_o^b\int_o^a (pw^2)dxdy \quad .....(3)$$

where ρ represents mass per unit area; and w is the time derivative of the transverse displacement w(x,y,t).

The total strain energy due to bending, U, is given by[3],[8]

$$U = \frac{D}{2}\int_o^b\int_o^a\{(w_{,xx})^2 + (w_{,yy})^2 + 2\nu w_{,xx}\, w_{,yy} + 2(1-\nu)(w_{,xy})^2\}dxdy \quad .....(4)$$

where D is the plate flexural rigidity. For a solid plate it is defined as

$$D = \frac{Eh^3}{12(1-\nu^2)} \quad .....(5)$$

for a hollow cellular plate as shown in Figure 1(c), and effective rigidity[7] will be used; thus

$$D = \frac{Esd^2}{2(1-\nu^2)} \quad .....(6)$$

The external work W due to a uniform pressure p(t) is given by

$$W = \int_o^b\int_o^a p(t)\, w\, dxdy \quad .....(7)$$

Substituting (1) into (3),(4),(7) and performing integrations; we then insert the final expressions for K,U, and W into the Lagrange equation (2) producing the modal equation of motion for all three cases; denoted by

$$\ddot{x} + \omega^2 x = C\, p(t), \quad .....(8)$$

whose details for the tree cases are :

Case (1) : x(t) is for $x_1(t)$

$$\omega = \left(\frac{D}{\rho}\right)^{1/2}\pi^2\left[\frac{1}{a^2} + \frac{1}{b^2}\right],\ C = \frac{16}{\rho\pi^2} \quad .....(9)$$

Case (2) : x(t) is for $x_2(t)$

$$\omega = \left(\frac{D}{\rho}\right)^{1/2}\pi^2\left[\frac{16}{3a^4} + \frac{1}{b^4} + \frac{8}{3a^2b^2}\right]^{1/2},\ C = \frac{8}{3\rho\pi} \quad .....(10)$$

Case (3) : x(t) is for $x_3(t)$

$$w = \left(\frac{D}{\rho}\right)^{1/2}\pi^2\left[\frac{12}{a^4} + \frac{12}{b^4} + \frac{8}{a^2b^2}\right]^{1/2},\ C = \frac{1}{\rho} \quad .....(11)$$

Therefore, the responses of plates can be determined provided that p(t) is given.

4. Dynamic Load Factors

As indicated by equation (8), a plate response will be approximately as a single-degree-of-freedom system. The results of such a system simplify the dynamic analysis. One approach for this consists of determining the static response and multiplying it by a dynamic load factor (DLF) to give corre sponding dynamic effects[2],[6]. The DLF is usually defined as the ratio of the dynamic response, x(t), to the static response, x_{st}. Since deflections and stresses in the plate are proportional, the DLF can be used in either. For equation (8), the pressure blast[5] p(t) is

considered to consist of a straight rise of pressure, with a rising time t_r, followed by an exponential decay, see Figure 2. Together with zero initial conditions, one should obtain the following expressions[4] for the DLF :

$$DLF = \frac{1}{t_r}\{\frac{t-\sin\omega t}{\omega}\}, \; t < t_r$$

$$DLF = \{\frac{k^2/\omega^2}{1+k^2/\omega^2} \quad \frac{\sin\omega t_r}{\omega t_r}\} \cos\omega(t-t_r) + \frac{e^{-k(t-tr)}}{1+k^2/\omega^2} + \{\frac{k/\omega}{1+k^2/\omega^2} + \frac{1-\cos\omega t_r}{\omega t_r}\} \sin\omega(t-t_r), \; t > t_r \quad .....(12)$$

It is clear that the DLF depends on time. A typical DLF is shown in Figure 3(a) while its maximum values (DLF_{max}) are plotted in Figure 3(b). These parametric curves represent DLF_{max} as a function of ω; they are given for some values of exponential decay k of the load.

5. Maximum Deflection and Maximum Stresses

First, the maximum static deflection, w_{st}, are determined by using equations (1) and (8). From (1) these occur at x = a/2 and y = b/2 for all three cases. Thus

$$\begin{aligned} &\text{Cast (1)} : w_{st} = x_{st} \\ &\text{Cast (2)} : w_{st} = 2x_{st} \\ &\text{Cast (3)} : w_{st} = 4x_{st} \end{aligned} \quad .....(13)$$

Where x_{st} is calculable from (8) by dropping out time-related terms. If we write p(t) as f(t). p_{max} and $f(t) \leq 1$ then the x_{st} is obtained :

$$x_{st} = \frac{C\, p_{max}}{\omega^2} \quad .....(14)$$

The dynamic deflection at this point is

$$w(a/2, b/2, t) = DLF(t).w_{st} \quad .....(15)$$

Its maximum value, w_{max}, is then determined by

$$w_{max} = DLF_{max}.\, w_{st}, \quad .....(16)$$

Where DLF_{max} can be found from the equation (12) for some t ; or some of DLF_{max} given in Figure 3(b).

Bending stresses[3],[7],[8] are considered as σ_x and σ_y :

$$\sigma_x = \frac{6D}{h^2}\left(\frac{\partial^2 w}{\partial x^2} + \nu\frac{\partial^2 w}{\partial y^2}\right); \quad .....(17)$$

$$\sigma_y = \frac{6D}{h^2}\left(\frac{\partial^2 w}{\partial y^2} + \nu\frac{\partial^2 w}{\partial x^2}\right);$$

Substituting (1) into this, and noting that ν is less than 0.5, and that the given plate geometry is b > 2a , the maximum stresses are obtained as follow :

Case (1) : It can be shown that the maximum bending stress will occur at mid-point of the plate, i.e., at x = a/2 and y = b/2 and that σ_x is the larger; being

$$\sigma_x = \frac{6D}{h^2}\pi^2\left(\frac{1}{a^2}+\frac{\nu}{b^2}\right).x_1(t)$$

Hence, its absolute maximum value is calculable from

$$(\sigma_x)_{max} = \frac{6D}{h^2}\pi^2\left(\frac{1}{a^2}+\frac{\nu}{b^2}\right).DLF_{max}x_{st} \quad .....(18)$$

Similarly, for the two following cases ;

Case (2) : The larger maximum stress is σ_x happening at the mid-span of clamped edges; being

$$(\sigma_x)_{max} = \frac{6D}{h^2}\left(\frac{4\pi^2}{a^2}\right).DLF_{max}x_{st} \quad .....(19)$$

Case (3) : The maximum stress is happening at x = a/2 and y = b/2 ; being

$$(\sigma_x)_{max} = \frac{6D}{h^2}8\pi^2\left(\frac{1}{a^2}+\frac{\nu}{b^2}\right).DLF_{max}x_{st} \quad .....(20)$$

These expressions for maximum bending stresses will be used for design purposes in checking for the stress limit that materials can bear.

6. Systematic Design Procedure

According to the details developed earlier a design procedure for the subpanels can be guidelined as follows :

(a) The pressure blast must be of the shape indicated by Figure 2. The rise time t_r and the exponential decay k must be given. The enclosure size must be given.

(b) The skeleton for rib structure must be decided, Figure 4, so that sizing of subpanels can be determined, i.e., dimensions "a" and "b" are selected to suit the supporting structure. Note also for $b > 2a$. The subpanel thickness "h" must also be chosen. The mechanical properties of the material used for the subpanels must also be clarified. They are modulus of elasticity E, Poisson's ratio ν, and the mass density ρ.

(c) Compute for the fundamental frequency ω as denoted by equations (9),or (10),or (11)

(d) Calculate and choose according to equation (12), or read from Figure 3(b), if possible, for the DLF_{max}.

(e) Compute for the maximum dynamic deflection w_{max} by using equations (13), (14), and (16).

(f) Compute for the maximum stress by using equations (18), or (19), or (20).

(g) Determine if the dynamic stress and/or deflection are acceptable by comparing with the prescribed design limits. If not, go on to stage (a) and revise the design.

Now, let us consider a sample design of which concerning data are displayed in Table 1. The input parameters and the design results are given in Table 2, Table 3, and Table 4.

7. Conclusions and Remarks

It can be seen from the sample calculations that there are number of cases that would be acceptable for practical design purposes. In general, as expected, when a resulting stress is large, the corresponding deflection tends also to be large. It is found out that results show zircaloy to have lower stresses but larger deflections than those of stainless steel. The hollow cellular stainless steel plates have additional stiffness, resulting in smaller deflections than those for a solid plate.

An eventual remark should be also stated that the approach considered in this study does not account for natural frequencies other than the fundamental one. If the pressure-blast frequency is considerable, it is meaningful to elaborate the study more on resonances that might happen.

8. Acknowledgement

The author would like to thank the Department of Mechanical Engineering, Chiang Mai University for allowing the lengthy calculations done on its computing facilities.

9. References

(1) Bares, R., "Tables for the Analysis of Plates, Slabs and Diaphragms Based on Elastic Theory," 2nd ed., Bauverlag GmbH.,Wiesbaden, 1971.

(2) Biggs, J.M., "Introduction to Structural Dynamics," McGraw-Hill, Inc., 1964.

(3) Langhaar, H.L., "Energy Methods in Applied Mechanics," John Wiley and Sons, Inc., New York, 1962.

(4) Meirovitch, L., "Analytical Methods in Vibrations," The Macmillan Co., New York, 1967.

(5) Peterson, R.R.; Moses, G.A., "Blast Wave Calculation in Argon Cavity Gas for Light Ion Beam Fusion Reactors," UWFDM-315, University of Wisconsin, 1979.

(6) Singer, F.L.; Pytel, A., "Strength of Materials," 3rd ed., Harper & Row, New York, 1980, p.p 528-534.

(7) Szilard, R., "Theory and Analysis of Plates," Prentice-Hall, Inc., New York, 1974.

(8) Timoshenko, S.P.; Woinowsky-Krieger, S., "Theory of Plates and Shells," 2nd ed., McGraw-Hill, Singapore, 1985.

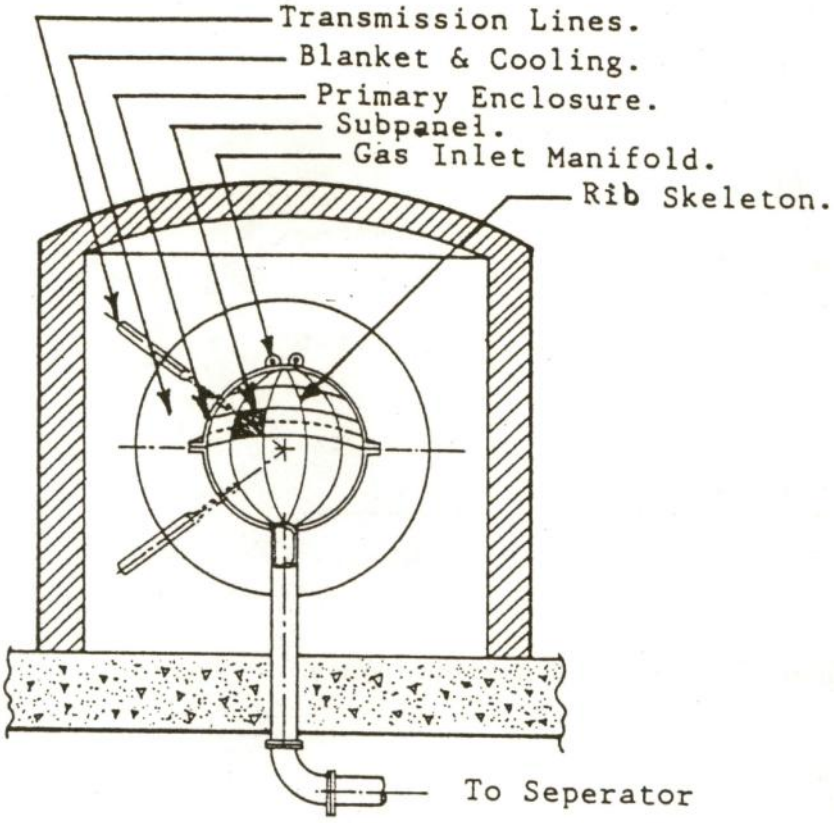

(a) Components of LIB Reactor.

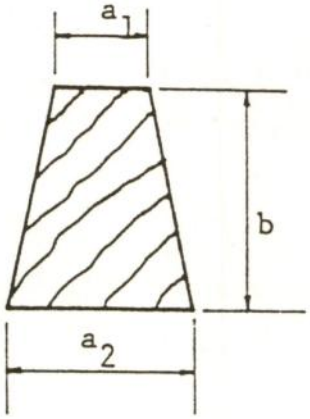

(b) Dimensions of Subpanels.

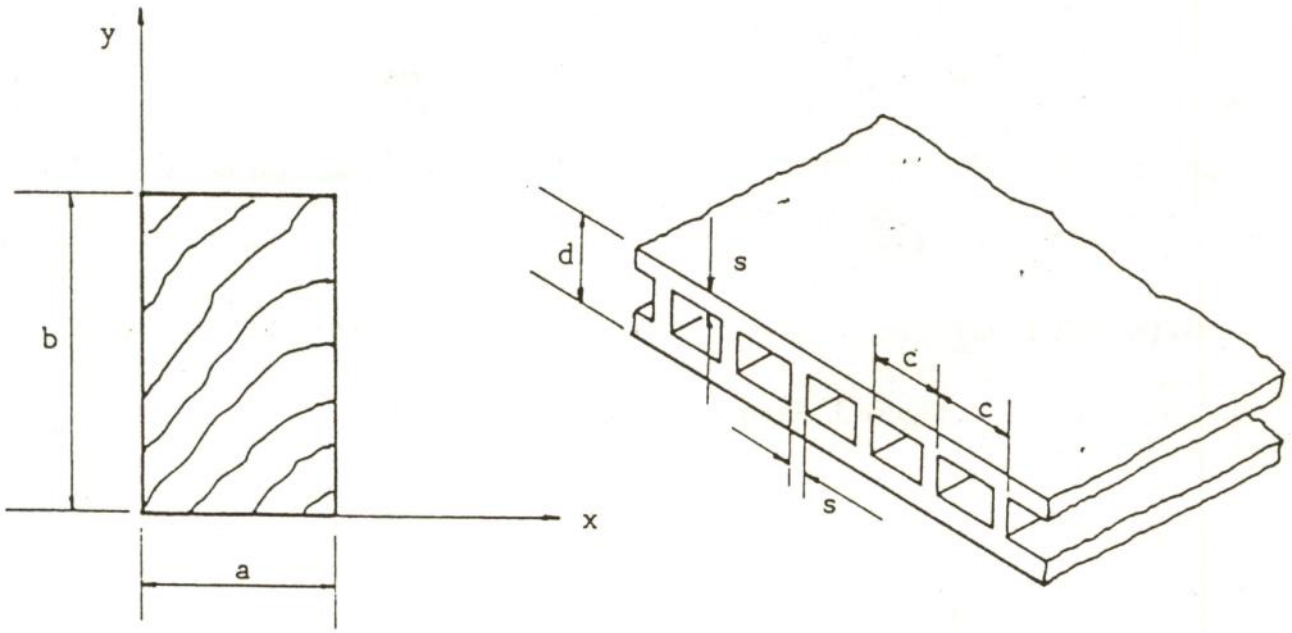

(c) Axes for Plate Analysis ; Thickness Details of Hollow Plate.

Figure 1. Sketched Details of LIB Reactor Cavity :

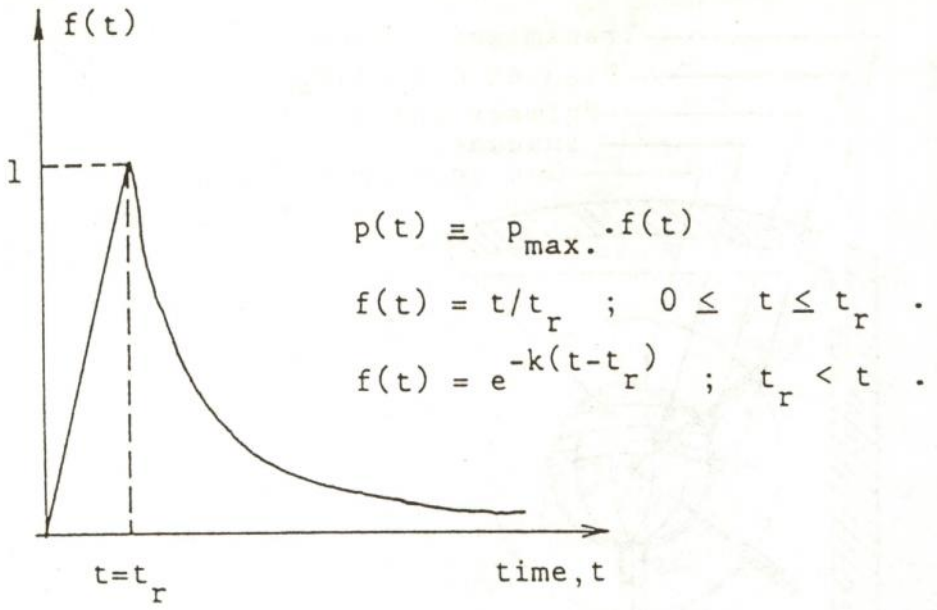

Figure 2. Representation of Blast Wave.

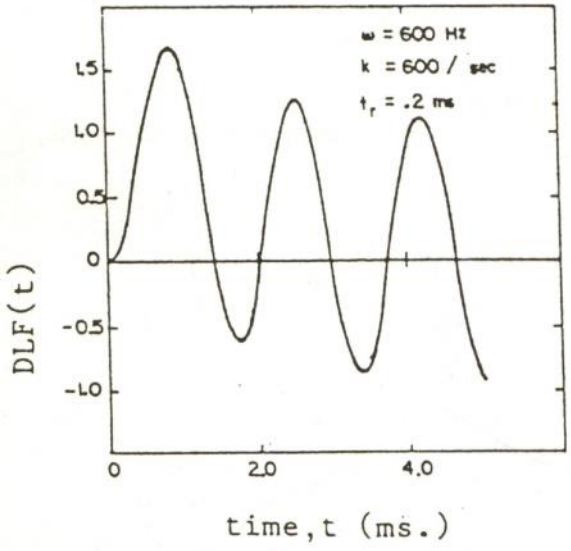

(a) Dynamic Load Factor.

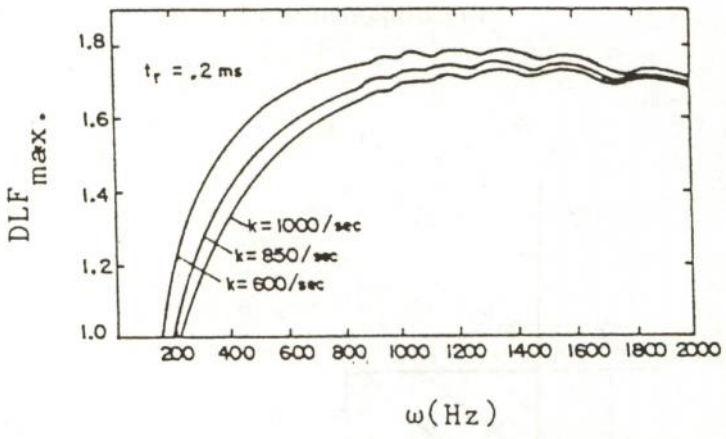

(b) Max. Dynamic Load Factors.

Figure 3. Sample Parametric Curves for DLF.

Figure 4. Hemispherical Ribbed Structure Used in Sample Calculation.

Table 1

Pressure Blast :

Maximum pressure, p_{max}	=	155	kPa.
Rise time, t_r	=	0.2	ms.
Exponential decay constant,k	=	600	$s^{-1.}$

Enclosure Size :

Shell radius	=	4	m.
Circumference	=	25.13	m.
Plate height, b	=	4.20	m.

Material for Shell :

Type of material : Solid stainless steel			
Density	=	8.027	Mg/m^3
Modulus of Elasticity, E	=	193.5	GPa.
Poisson's ratio, ν	=	0.33	
Allowable working stress, σ_w	=	200	MPa.
Type of material : Solid zircaloy			
Density	=	6.440	Mg/m^3
Modulus of Elasticity, E	=	76.0	GPa.
Poisson's ratio, ν	=	0.33	
Allowable working stress, σ_w	=	138	MPa.

Edge Conditions :

Simply supported edges parallel to the equator.
Clamped edges along the meridian.

Table 2

Input Parameters and Results for Solid Stainless Plate with Edge Supports as indicated in Table 1.

Choices of Design	Meridian lines	"a" (m)	b/a	"h" (mm)	"w" (Hz)	DLF_{max}	$(6x)_{max}$ (MPa)	w_{max} (mm)
(a)	24	0.524	8.02	10	200	1.20	197	2.50
(b)	28	0.449	9.36	10	270	1.36	163	1.52
(c)	20	0.628	6.68	15	210	1.24	129	1.60
(d)	24	0.524	8.02	15	300	1.41	103	0.85
(e)	12	1.047	4.01	20	100	1.00	159	4.08
(f)	16	0.785	5.35	20	180	1.12	102	1.34
(g)	20	0.628	6.68	20	277	1.37	81	0.77
(h)	12	1.047	4.01	25	126	1.00	102	2.10
(i)	16	0.785	5.35	25	220	1.26	74	0.88

Table 3

Input Parameters and Results for Solid Zircaloy Plate with Edge Supports as indicate in Table 1.

Choices of Design	Meridian lines	"a" (m)	b/a	"h" (mm)	"ω" (Hz)	DLF_{max}	$(\sigma_x)max$ (MPa)	w_{max} (mm)
(a)	24	0.524	8.02	10	139	1.00	164	5.30
(b)	28	0.449	9.36	10	190	1.18	141	3.42
(c)	20	0.628	6.68	15	146	1.00	103	3.30
(d)	24	0.524	8.02	15	209	1.22	89	1.83
(e)	12	1.047	4.01	20	71	1.00	159	10.40
(f)	16	0.785	5.35	20	125	1.00	91	3.28
(g)	20	0.628	6.68	20	194	1.20	70	2.00
(h)	12	1.047	4.01	25	86	1.00	109	5.50
(i)	16	0.785	5.35	25	156	1.10	65	1.93

Table 4

Input Parameters and Results for Hollow Cellular Stainless Plate with Edge Supports as indicated in Table 1. and c = 2d, h = d.

Choices of Design	Meridian lines	"a" (m)	b/a	"d" (mm)	"s" (mm)	"ω" (Hz)	DLF_{max}	$(\sigma_x)max$ (MPa)	w_{max} (mm)
(a)	20	0.628	6.68	20	2.27	480	1.60	58	0.79
(b)	24	0.524	8.02	20	1.67	690	1.71	41	0.52
(c)	20	0.628	6.68	30	1.62	720	1.72	26	0.49
(d)	24	0.524	8.02	30	1.17	1035	1.78	18	0.33
(e)	20	1.628	6.68	40	1.25	960	1.77	15	0.36
(f)	24	0.524	8.02	40	0.88	1380	1.79	10	0.25
(g)	12	1.047	4.01	50	2.44	455	1.58	25	0.89
(h)	16	1.785	5.35	50	1.52	770	1.73	15	0.46
(i)	20	0.628	6.68	50	1.01	1200	1.79	9	0.28